

## INVESTIGATION OF HAGC SYSTEM PERFORMANCE WITH VARIOUS CIRCUITRY DESIGNS

Remn-Min Guo, Tenova I2S  
Tony Manias, Tenova I2S  
475 Main St, Yalesville, Connecticut 06492  
Phone 203-265-5684, Fax 203-284-1819, e-mail: RGuo@i2s.com, [AManias@i2s.com](mailto:AManias@i2s.com)

**Keywords:** Hydraulic system, AGC, Gage Control, Response Time, MATLAB

### INTRODUCTION

The Hydraulic Automatic Gauge Control (HAGC) is one of the most important systems in a rolling mill to guarantee the gage performance. Since 1960 when the servo systems were introduced for heavy duty control in the metal industry, the HAGC system has become an essential part of rolling mill design. Engineers and scientists with knowledge in mathematical modeling, control theory, and programming skill have dedicated their efforts to accomplish a common goal of a better HAGC system. In addition, hydraulic manufacturers have improved their products to work with mill designers for better system performance with a lower cost. The intention of this article is to evaluate the system performance by combining recent advances of hardware (hydraulic components) and software (control system and mathematical models) in this field.

Although overall gage accuracy relies on mechanical, electrical, hydraulic, control system designs, and even the product mix, the hydraulic system response plays a key role on the performance of the entire system. The earliest studies in the servo system was limited on a light duty mechanism with nearly zero spring force in early 60's<sup>[1,2]</sup> of last century. During the next decade, the hydraulic system response had been researched<sup>[3-6]</sup> and innovative control concepts<sup>[7-10]</sup> had been implemented into production mills. Better understanding of the system response from various rolling parameters led to a better system design. Although many technical aspects were resolved by previous studies in the blooming 80's<sup>[11-14]</sup>, there are still some unclear issues affecting the system performance, such as, the friction force, internal oil leakage, the return line design, the piston to rod area ratio, and the selected servo valve size. In early 1990's, Guo extended Paul's model<sup>[5]</sup> to combine servo valve, transmission line, hydraulic cylinder, mill dynamics, returning line, and sensor response in a state space matrix which was solved using 4<sup>th</sup> order Runge Kutta numerical method<sup>[15]</sup>. At the turn of this century, more research works were developed in the academia. For instance, Suisse<sup>[16]</sup> presented an analytic model for dynamic seal friction in hydraulic actuators as a function of cylinder pressure, seal material, piston rod dimensions, piston rod seal gland dimensions, and other influencing factors. This study did not show the response of the entire hydraulic AGC system. Gao<sup>[17]</sup> et al developed a simplified model specifically for a 1100mm cold mill and compared the results with mill data; however, no performance comparison was provided. Rath<sup>[18]</sup> summarized the control system of cold rolling, but did not have detailed discussion on different responses due to various rolling parameters. Stefan<sup>[19]</sup>'s model focused on the position and force modes of the control system, hence, the hydraulic system was simplified and the relations between rolling force and the exit gage were emphasized in his model.

Presented in this article is a continuous development from Guo's previous work<sup>[15]</sup> to investigate the hydraulic system response considering mill dynamics, servo-valves, hydraulic cylinder, transmission pipe line, returning line, sensors, and other necessary components. All differential equations in Laplace domain are shown in the first section. After linearizing three nonlinear equations, a closed form transfer function of the displacement to the input signal was derived by solving nine equations simultaneously. However, the closed form is too complicated to transform inversely back to the time domain, neither to provide any further information of system performance. The software package MatLab was employed to take advantages of its simulation capability as well as its graphic expressions of all related parameters. An overall block diagram is presented to link with the associate package SimuLink of MatLab. All nonlinear solutions were obtained from SimuLink. The frequency response of the linear system will be shown in Section 2, followed by the result comparison of both linear and non-linear models in Section 3. As expected, the nonlinear terms do not impose large response differences to the system from the comparison results. System performances due to the nonlinear terms, such as friction force, returning pipe line length, piston internal leakage, and piping systems are studied and the results are placed in Section 4. The study shows that friction force is a damping force to the system. The larger friction force does not hamper the system response, but reduce the ring of the system. It should be a major component of mill chatter vibration control. The pipe friction force of the returning line generates a back pressure to against the piston movement. According to the study, although this friction force is qualified to be a damping force to the cylinder, it is by no means a damping force to the complete hydraulic system. The internal leakage through the piston drives the system to other convergent position but the target in the step response. The system remains very stable after all even with a very high current gain factor. The frequency responses using three different piping systems are demonstrated using the Bode diagrams. In general, the system without connecting the rod side to the servo valve provides better frequency response in any combinations of rolling parameters.

## THEORETICAL DERIVATION

The primary objective of this article is to evaluate the system performance with various frictions, leakages, and pipe lengths. The performance of using three piping circuitries will be evaluated. The investigation includes different usage of the four ports of the servo valve, various pipe line parameters and configurations, and the hydraulic cylinder designs and characteristics.

The hydraulic system is composed of the servo-valve, the transmission line from the servo valve to the cylinder, the cylinder, and the return line back to the tank. For a single acting cylinder, Paul<sup>[4,5]</sup> developed a mathematical model to examine the performances with various transmission line lengths. The entire hydraulic system is governed by physical different equations based on the system design. The following equations were expanded from Paul's study according to a typical HAGC hydraulic system design with one servo valve. The equation set also assumes that the oil pressure in the piston side increases when charging from the system pressure and the pressure decreases when dumping the oil to the tank. The rod side has no connection with the servo valve. The characteristic of the servo valves can be obtained from Moog<sup>[20]</sup> technical bulletin. The mill dynamics equation adopts Guo's method<sup>[15]</sup> to apply the mill natural frequency<sup>[21,22]</sup>, the damping force<sup>[23]</sup>, and the equivalent mill modulus for the equivalent mass, the damping coefficient, and the spring constant of the mill. In the later section, some equations as shown below were modified, added, or eliminated to fit with the specific conditions of the investigation cases.

### Basic Equations of Hydraulic System

The differential equations in Lapace domain can be summarized in the followings:

- |     |                                 |  |
|-----|---------------------------------|--|
| 1)  | Servo valve spool dynamics      | $s^2c + 2\xi\omega_s sc + \omega_s^2c = \omega_s^2I_c$                           |
| 2)  | Servo valve input current       | $I_c = K_c(u_y - u_x) / I_0$   |
| 3)  | Servo valve flow rate           | $q = q_{r0}c\sqrt{\Delta P / \Delta P_0}$  |
| 4)  | Transmission line flow          | $q = q_a + K_t sP$   |
| 5)  | Transmission line pressure drop | $P - P_a = K_p s q_a + R_p q_a$  |
| 6)  | Piston side pressure change     | $sP_a = \beta_e (q_a - A_a s x - K_l (P_a - P_b)) / (V_0 + A_a x)$               |
| 7)  | Rod side pressure change        | $P_b = P_{b0} + K_r s^2 x + R_r s x$   |
| 8)  | Mill Force Equilibrium          | $2(P_a A_a - P_b A_b) = m s^2 x + b s x + k_m x + f_c \text{sgn}(\dot{x}) + f_x$ |
| 9)  | Position Sensor                 | $\tau_x s u_x + u_x = x$   |
| 10) | Equivalent Oil Bulk Modulus     | $1/\beta_e = 1/\beta_0 + (1-2\nu)d_p / (Et_p) + \eta_{air} / \beta_g$            |
| 11) | Equivalent Mill Modulus         | $1/k_m = 1/k_{m0} + L_a / (\beta_e A_a)$   |

where

$c$	servo valve opening	$\omega_s$	natural frequency of servo valve
$K_c$	servo valve current gain	$u_y$	desired position input
$u_x$	position feedback	$I_0$	rated servo valve current
$q_{r0}$	rated servo valve flow rate	$\Delta P$	pressure drop
$q$	flow rate through the servo valve port	$q_a$	flow rate into cylinder (piston side)
$K_t$	$=A_p L_p / \beta_e$ , a transmission line factor	$A_p$	cross section area of transmission pipe
$L_p$	length of transmission pipe	$\beta_e$	equivalent bulk modulus of oil
$P$	pressure at the servo valve port	$P_a$	pressure at the cylinder (piston side)
$K_p$	$=\rho L_p / A_p$ , piston side pressure drop coefficient	$\rho$	oil density
$R_p$	$=8\pi\mu L_p A_d / A_p^2$ , piston side pressure drop coefficient	$L_{rp}$	length of return line
$\mu$	oil viscosity	$A_b$	rod side area
$A_r$	cross section area of returning pipe	$A_a$	piston side area
$x$	piston displacement	$K_l$	oil leakage coefficient
$V_0$	initial cylinder volume	$P_b$	pressure at the cylinder (rod side)
$P_{b0}$	pressure at the end of the return line (or tank)	$K_r$	$=\rho L_r A_b / A_r$ , rod side equivalent mass coefficient
$R_p$	$=8\pi\mu L_{rp} A_b / A_r^2$ , rod side pressure drop coefficient	$m$	equivalent mill mass
$b$	equivalent mill damping coefficient	$k_m$	equivalent mill modulus
$f_x$	imposed force to the cylinder	$\tau_x$	position sensor time constant
$\beta_0$	oil bulk modulus	$\nu$	pipe material Poisson ratio
$d_p$	pipe inner diameter	$E$	pipe material Young's modulus

$t_p$	pipe wall thickness	$\eta_{air}$	air ratio in the pipe line
$\beta_g$	air bulk modulus	$k_{mo}$	mill modulus
$L_a$	oil column (piston side)	$f_c$	friction force in the cylinder

The dynamic behavior of the hydraulic transmission lines is a distributed system depending on space and time<sup>[5]</sup>. It can be characterized by partial differential equations or by ordinary differential equations. Partial differential equations are better approximation but they are not easy to be engaged with the total hydraulic system and therefore ordinary differential equations are used on this article. Equations 4 and 5 are applied to study the transmission line effect.

The initial condition at  $t=0$  is  $I_c=0$ ,  $u_{y0}=u_{x0}$ ,  $c=0$ ,  $dP_a/dt=0$ ,  $q_{a0}=q_0=0$ ,  $x=x_0$ ,  $dx/dt=0$ ,  $d^2x/dt^2=0$ , and  $f_x=f_{x0}$ . Refining variables  $x$ ,  $P_a$ ,  $P_b$ ,  $P$ ,  $u_x$ ,  $u_y$ , and  $f_x$  as  $x-x_0$ ,  $P_b-P_{b0}$ ,  $P_a-P_{a0}$ ,  $P-P_0$ ,  $u_x-u_0$ ,  $u_y-u_0$ , and  $f_x-f_{x0}$  respectively, the above equations can be normalized so as to zero all initial conditions. Most equations stay the same except equations (6) ~ (8) have slightly modifications which can be seen from the block diagram as shown in Figure 1.

### Solution of Linear Equations

Equation (3) is non-linear and  $\Delta P$  depends on the sign of  $c$ ;  $\Delta P=P_s-P$  for  $c>0$  and  $\Delta P=P-P_t$  for  $c<0$ , where  $P_s$  is the system pressure (or the accumulator pressure) and  $P_t$  is the tank pressure. As proposed by Paul<sup>[4]</sup>, Equation (3) can be linearized using Taylor's expansion with the average values for the partial differential terms, namely

$$(12) \quad q = q_{r0}c\sqrt{\frac{P_s-P}{500}} \approx Q_c c + Q_p P \quad \text{where} \quad Q_c = \frac{\partial q}{\partial c} = q_{r0}\sqrt{\frac{P_s-P_{avg}}{500}} \quad \text{and} \quad Q_p = \frac{\partial q}{\partial P} = -\frac{q_{r0}c_{avg}}{\sqrt{500(P_s-P_{avg})}}$$

Besides of the above linearized equation (12), the following assumptions are required to achieve a linear equation set:

- no oil leakage in the cylinder,  $K_l=0$
- the initial cylinder volume  $V_o$  is much larger than the volume due to  $x$  so that  $V_o+A_a x \approx V_o$
- no cylinder friction,  $f_c=0$
- the external force  $f_x$  is a constant, which has no relationship with other parameters

### Derivation of Linear Solution

Equations (6), (7) and (8) can be simplified and combined to solve for  $x$  as a function of  $q_a$ :

$$(13) \quad x = \gamma q_a \quad \text{where} \quad \gamma = 2\alpha A_a / (n_3 s^3 + n_2 s^2 + n_1 s)$$

$$n_1 = m + 2K_r A_b \quad n_2 = b + 2R_r A_b \quad n_3 = k_m + 2\alpha A_a^2$$

On the other hand, equations (1) ~ (3),  $q$  can be solved as a function of  $u_x$  and  $P$  which can be rewritten as a function of  $q_a$  and  $x$ . Combining the rewritten forms of  $q$  and  $P$  together with equations (4) and (9), one can get the flow rate  $q_a$ :

$$(14) \quad q_a = z_1 u_y + z_2 x$$

where

$$z_1 = \frac{Q_c K_c \omega_s^2}{I_o (s^2 + 2\xi \omega_s s + \omega_s^2) (1 + \alpha K_t + s K_t (s K_p + R_p))} = \frac{C_{z1}}{\sum_{i=0-5} v_i s^i}$$

$$C_{z1} = Q_c K_c \omega_s^2 / I_o$$

The other part  $z_2$  can be expressed as

$$z_2 = \frac{\alpha A_a (s K_t - Q_p) s}{D(s)} - \frac{C_{z1}}{(s \tau_x + 1)(s^2 + 2\xi \omega_s s + \omega_s^2) D(s)} = \frac{\sum_{i=0-5} w_i s^i}{\sum_{i=0-6} m_i s^i}$$

$$\text{where} \quad D(s) = K_t K_p s^3 + K_t R_p s^2 + (1 + \alpha K_t) s - Q_p (K_p s^2 + R_p s + \alpha)$$

The coefficients of  $v_i$ ,  $w_i$ , and  $m_i$  can be obtained easily and will not be reiterated here. Inserting (14) into (13), one can solve the displacement  $x$  explicitly as a function of  $u_y$  (transfer function):

$$(15) \quad \frac{x}{u_y} = \frac{\gamma z_1}{1 - \gamma z_2} = \frac{z_1}{\gamma^{-1} - z_2} = 2\alpha A_a Q_c C_{z1} \frac{\sum m_i s^i}{[\sum v_i s^i][(\sum n_i s^i)(\sum m_i s^i) - 2\alpha A_a w \sum m_i s^i]}$$



The length of the transmission line is one of the most important factors affecting the hydraulic response. When the servo valve is mounted directly on the cylinder, the length of the transmission line is almost zero and therefore the hydraulic system response is improved. Nowadays most of the applications are designed based on the assumption that the transmission line is so short that it can be eliminated from the hydraulic system equations. However in some revamping applications, the roll force cylinders are built to fit into the mill housing screw cavity and the servo valve cannot be mounted directly to the cylinder. A transmission line is required for this special condition. Figure 2 shows the cylinder frequency response with two different transmission line lengths. Friction force and internal leakage are not considered in this case.

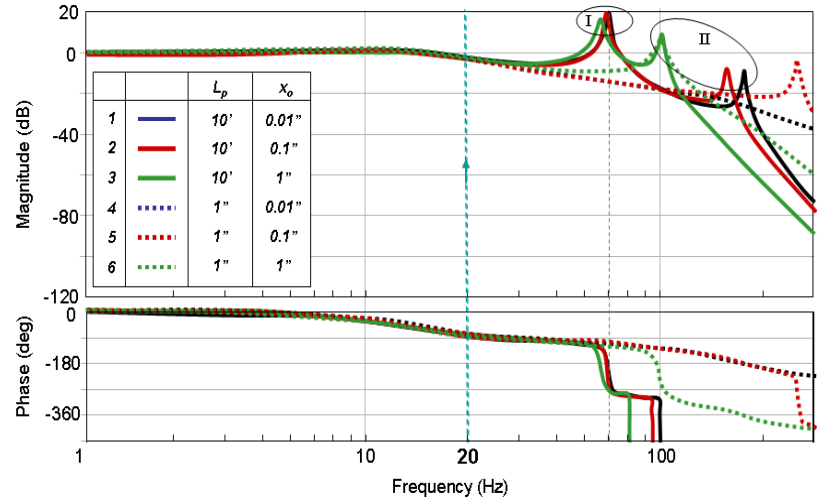


Figure 2: Bode Chart for Hydraulic System Response

There are six studies for various transmission pipe line lengths and the initial oil columns. Figure 2 shows the Bode diagrams of all six cases. Two groups for the transmission line lengths – the solid lines are for the long length (10') while the dotted lines are for the short length (1'). It takes a longer time for the pressure wave to travel from the servo valve to the hydraulic cylinder for a longer transmission line<sup>[15]</sup>. Hence, the better system performance is expected for shorter transmission line cases.

Within each transmission line length group, there are three cases for various initial oil columns – the blue one is for a small column (0.01"), the red one is for the medium column (0.1"), and the green one is for the large column (1"). The larger oil column results in the smaller oil spring constant due to greater oil compressibility. Hence, the system should have a slower response for the larger initial oil column since more oil is needed to boot up the cylinder pressure during the charging cycle and to pump out more oil during the dumping cycle.

For the cases of 10' transmission line, Figure 2 shows two natural frequency groups. The frequencies of the first group are very close to the mill natural frequency of 64 Hz although Eq. (15) does not show the mill natural frequency as a pole of the system explicitly. The second group has the frequencies from 100 Hz to 200 Hz, which are close to the valve natural frequency of 160 Hz. Again, this natural frequency cannot be observed from Eq. (15). It asserts that the larger oil column causes the lower natural frequency, which may affect the desired mill speed, but no trivial effects on the system response. The performances for the operation frequency of 20 Hz have shown nearly no difference. The magnitude is about -3 db and the phase angle is about 80° for all cases, which matches with Stone's suggestion<sup>[6]</sup>. The chart also shows an overshoot slightly at the lower frequency zone, which can be eliminated by lowering down the current gain of the servo-valve.

As to the 5<sup>th</sup> and 6<sup>th</sup> cases with a short transmission line only 1" (such as direct mounted to the cylinder), the first natural frequencies are delayed to be higher and the second natural frequencies are greater than 300 Hz (not shown in Figure 2). There are no natural frequencies found within 300 Hz for the small oil column case (case 4). Hence, Figure 2 concludes that both transmission line length and the initial oil column have no trivial effects on low frequency operation (20 Hz), but have observable effects on the natural frequencies of the system. The initial oil column has larger effect than the transmission line length.

### NON-LINEAR SYSTEM AND NUMERICAL SOLUTIONS

The previous linear study demonstrates the hydraulic system can perform a satisfactory response without considering many non-linear effects. The following sections will investigate the non-linear system with various conditions, such as the cylinder friction force, the cylinder internal leakage, the area ratio of two sides of the cylinder, and various piping arrangements, which cannot be simulated using the linear

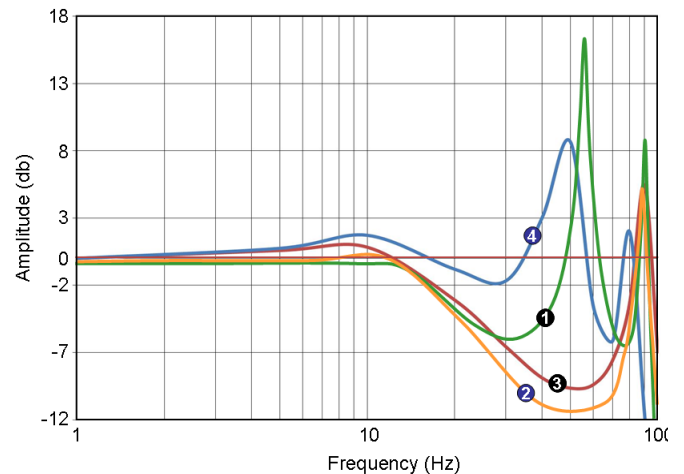


Figure 3: Frequency Response Comparison for Linear and Non-Linear Systems

approach.

The Servo valve flow rate (Eq. 3) is a non-linear equation and it deserves more attention in order to get more accurate results. The flow rate  $q$  is proportional to the valve opening  $c$  and it is also determined by the pressure drop between two ports of the servo valve. Using Taylor's expansion and neglecting the high order terms, the square root portion can be linearized (see Eq 12). However, since the pressure drop changes every time the spool alternates its position, the system remains non-linear. According to the spool position, Equation (3) will be rewritten as

$$(16) \quad q = \begin{cases} q_{r0} c \sqrt{(P_s - P_1) / \Delta P_0} & c > 0 \\ q_{r0} c \sqrt{(P_2 - P_r) / \Delta P_0} & c \leq 0 \end{cases}$$

where  $\Delta P_0$  is a reference pressure drop depending on the piping arrangement. It equals to 1000 psi if two ports A and B are applied; and 500 psi if only one port is used. The piston side pressure change (Eq. 6) is another non-linear equation because the displacement  $x$  is included in the denominator. In order to have a rational comparison between linear and nonlinear solutions, the initial pressures of  $P_s$ ,  $P$ , and  $P_t$  are set at 5000 psi, 2600 psi, and 200psi respectively so that the pressure drops of both charging and dumping conditions become the same. This setting will reduce the tendency of uneven response from the system due to difference flow rate from the servo valve. Except this small data modification, other data are identical to the data applied in the linear study. Figure 3 shows the magnitude curves (in db) of the Bode charts from the linear and non-linear systems for comparison. For convenience, the study will focus on the mill operating frequency range of less than 100 Hz henceforward. The linear cases are shown in curves ① and ③ while the nonlinear cases are shown in ② and ④. All four cases have the same initial oil column of 1", which is for a long stroke cylinder. The cases ① and ④ have a longer transmission line (10') than other two cases (only 1'). Other parameters are the same for all cases.

Obviously, the nonlinear terms do not impose a large effect on the magnitude for the frequency less than 20 Hz. Some differences are shown in the overshoot. Once the current gains are adjusted individually, the response is expected to be very close at the low frequency ( $\leq 20$  Hz) range. The nonlinear terms do cause the natural frequencies occurred earlier and generate less positive amplitude response, which is not significant in the mill operating range however.

### CASE STUDIES WITH NONLINEAR EFFECTS

Previous two sections focus on the system response of the linear system as well as the performance comparison of linear and nonlinear systems. The non-linear term of the servo valve flow rate was used to make comparison of the system response. The piston and rod side pressures were so designed specially that the charging ( $c > 0$ ) and dumping ( $c < 0$ ) responses were nearly the same. This section will discuss about other nonlinear effects – friction force, returning line, and internal leakage. It is important to note that the linear system can be used to design the controller for better system performance in the future study. Understanding of nonlinear effects facilitates the design of the controller of the linear system.

#### Friction Force Effect

It is well known that friction force is a resistance force opposite to the movement of one object against another. It is always in a direction against actuator motion; and therefore it switches direction with the velocity of the piston  $\dot{x}$  as shown in Eq. (8). This section investigates the system response to the step signal for various initial oil columns and the transmission line lengths. The static friction force is considered here for the step response. Although the dynamic friction force should be considered after the piston starts to gain the velocity, this study assumes the static friction force be the same during the step response test.

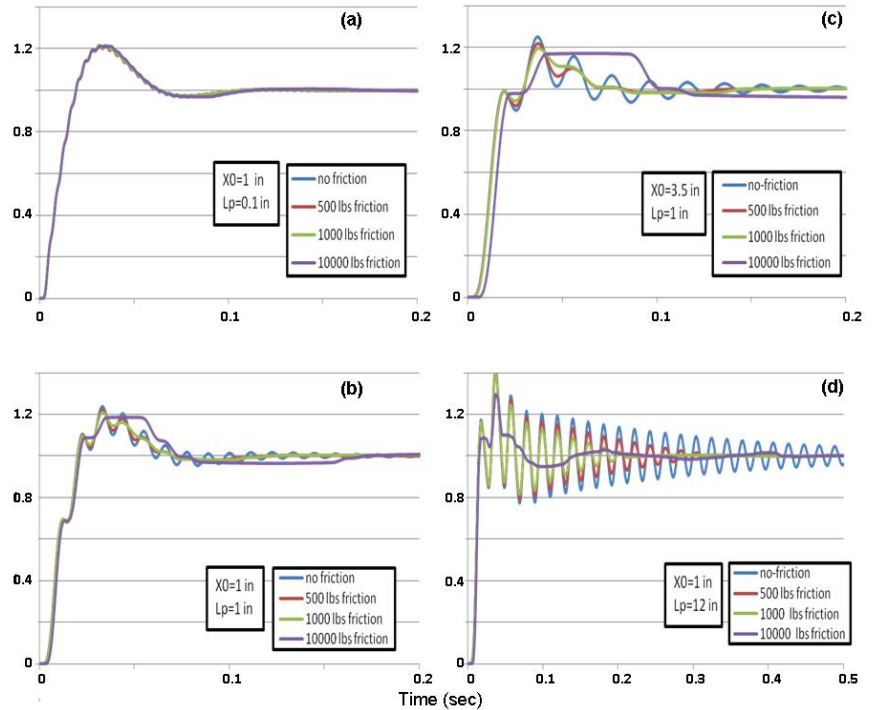


Figure 4: Friction Force Effects

As shown in Figure 4a, for a small oil column, such as the so-called pancake cylinder with a very small stroke or a long stroke cylinder with the maximum roll configuration, the friction forces have nearly no effects for all cases. Figure 4a also shows a small delay at the beginning to conquer the system inertia and the static friction force. After this delay, the system has 20% overshoot and stabilizes after about 0.1 second. The overshoot can be modified by lowering the servo valve gain factor. The response curves for larger friction forces show a very small fluctuation.

For the cases with 1" initial oil columns, Figure 4b shows that the response curves follow the curve with 0.1" oil column very well. However, the fluctuation becomes larger and takes about 0.18 sec to eliminate the ripples. The friction force serves as a damping force to reduce the fluctuation. The larger the friction force is, the smaller the amplitude and the less ring time becomes. Nearly no wave forms are found for the cases with friction forces  $\geq 1000$  pounds. Figure 4c shows that the system rings after 0.2 second for the cases with large initial oil columns and insufficient friction forces. The response curves have no apparent ripples if the friction force reaches 1,000 pounds and beyond. The amplitude of the ripple is inversely proportional to the friction force. Figure 4d and 4b can be used to examine the effect due to the transmission line length. The larger transmission line length enlarges the amplitude of the response curves although the systems are still stable. The case with the highest friction force still has a very smooth response curve and converges after 0.2 second thanks to the large damping force.

Consequently, Figure 4 concludes that a proper system friction force facilitates the stability with slightly sacrifice of the response time. The friction force  $f_c$  as shown in Eq (8) is in fact a damping force to the rolling mill equilibrium condition and it is also a qualified damping force for the entire hydraulic system.

### Returning Line Effect

On the other hand, the back pressure on the rod side could be a kind of damping force as well. With the commercial hydraulic system design, the oil in the returning line is of a laminar flow with a cylinder speed in the mill operating range. Hence, the friction force in the return line is a linear function of the oil speed in the pipe line, which is proportional to the piston speed according to the mass conservation law. The downward movement of the piston will impel the oil out of the rod side to the returning line, which tends to increase the back pressure (due to the pipe friction force) to against the piston movement. The higher speed causes the larger friction force proportionally. The upward movement of the piston will suck the oil back to the rod side, which generates a friction force to drag the piston movement. Accordingly, the friction force in the returning line is proportional to the piston speed and also against the piston movement, which is a sufficient condition of a damping force.

As shown in Eq. 7, the friction force in the returning line is a function of  $K_r$ , which is proportional to the line length and the ratio of the rod side area to the pipe inner area. Figure 5 shows step and frequency responses for various return line lengths. Here the pipe length is applied so as to keep the oil speed in the pipe line the same for all cases and the oil in the returning line will maintain the same state of the laminar flow. The pipe line diameter is not changed since the smaller pipe inner diameter increases the oil speed in the pipe line, which may change from laminar to turbulent flow and alter the friction coefficient in the returning line. Besides of varying the length of the return line, some parameters used in this investigation are  $P_s=5000$  psi,  $P_r=15$  psi,  $P_{a0}=3600$  psi, and  $P_{b0}=200$  psi while other parameters remain the same.

Figure 5 shows the step and frequency responses for the returning line lengths of 10', 15' and 50'. The friction force is greater for the longer returning line according to Eq. 7. However, Figure 5a shows that the system rings more for the longer returning line, which implies that the friction force in the returning line cannot be a damping force although its behavior to the piston is qualified to be a damping force. Figure 5b shows the frequency response curves of various returning lines with input frequency of 20 Hz. The interesting viewpoint is that the longer return line with higher back pressure (friction force) provides a better frequency response. The phase angles for all three cases are about the same except that the 50' case has a slightly smaller phase angle (not shown in Figure 5). Figure 5 confirms that the returning line cannot serve as a damping force, but it can improve the frequency response. The linear solution also shows similar results on the friction force in the returning line.

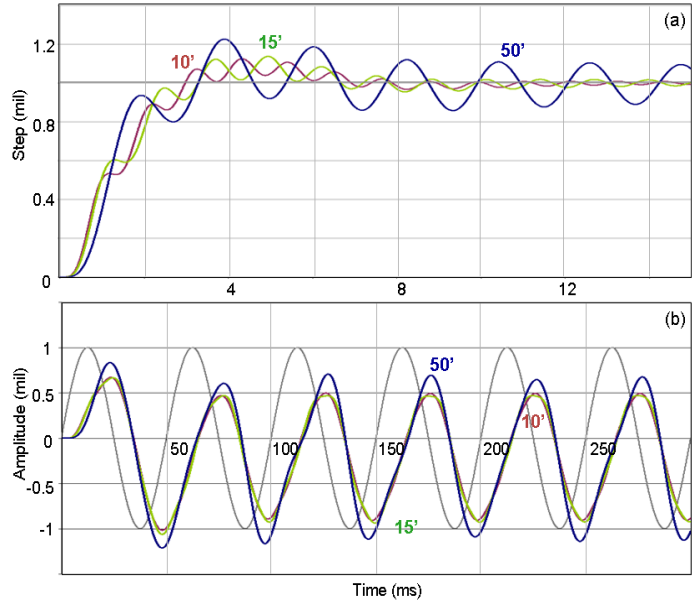


Figure 5: Step Response due to Various Return Line Lengths

The larger transmission line length enlarges the amplitude of the response curves although the systems are still stable. The case with the highest friction force still has a very smooth response curve and converges after 0.2 second thanks to the large damping force.

### Leakage Effect

The cylinder leakage is another constitutive parameter of the non-linear hydraulic system. There are two types of leakages in a hydraulic system - the internal and the external leakages. The external leakage can be easily determined with a quick visual inspection of the hydraulic cylinder rod. The internal leakage test cannot be done that easy and the use of a hand held ultrasonic tester is needed<sup>[24]</sup>. This sub-section is used to examine the step response of various internal leakages through the piston. The system response can be used as an indicator of internal leakage.

The leakage coefficient  $K_l$  is assumed here ranging from 0.001 to 0.005 so as to observe response differences. In addition to varying leakage coefficients, other parameters used in this investigation are the same as the previous case. Leakage from the piston side to the rod side due to the pressure difference will cause the pressure drop in the piston side due to oil leakage. Hence, the servo valve needs pump in more oil to compensate for oil leakage and to increase the pressure at the piston side. At the same time, if the rod side is connected to the tank (see Figure 7b), the excessive oil from the piston side will dump back to the tank, which will not increase the rod side pressure.

Figure 6a shows the step response curves for various leakage coefficients. The input signals for all cases are the same 1 mil. The system will reach the target position of 1 mil after 70 ms if the system has no leakage. However, as the leakage coefficient increases, the system converges to other positions depending on the leakage coefficient. The higher leakage coefficient causes the larger pressure drop in the piston side regardless of the larger position error to the servo valve. The resultant pressure at the piston side cannot overcome the imposed rolling force due to continuous leakage through the piston. Eventually, the system converges to a lower position than the desired position:

$K_l$	Final Position (mil)
0.001	0.85
0.002	0.70
0.003	0.55
0.005	0.26

The above table shows that the final convergent position is very close to a linear function of the leakage coefficient. It is about 0.15 mil position drops per 0.001 leakage coefficient increments.

The current gain of the previous case was set at 4000. Is there a possibility to increase the current gain so as to push the response curve back to the target of 1 mil? Figure 6b shows the response curves for various current gains acting on the case of leakage coefficient of 0.001. The results can be summarized as 70% response for the gain of 2000; 80% for 3000, 90% for 5000, and 92% for 8000. The higher gain factor generates larger ripples, but the system converges stably. However, the system cannot reach the target even with a larger current gain.

Figure 6c shows a step response curve with an extremely high current gain of 30,000. The purpose is to test the current gain limit to see if the system will become unstable. The curve shows that the system can be stable after about 200 ms and it does converge to the target. Note that the servo valve could be saturated for such a large displacement, which is not considered in the model. Figure 6 does not show the saturation condition of the servo valve. The huge amplitude fluctuation between -1.5 and 3.5 is too large to be acceptable for the system design. The conclusion is that the internal leakage hampers the system response regardless of the current gain of the servo valve.

### System Responses for Three Different Hydraulic Piping Designs

So far, all studies consider only one port (A) of the servo valve is used and the other port (B) is plugged. The servo valve is connected only with the pressure side of the cylinder and the rod side of the cylinder is piped directly to the tank. In this case a low pressure

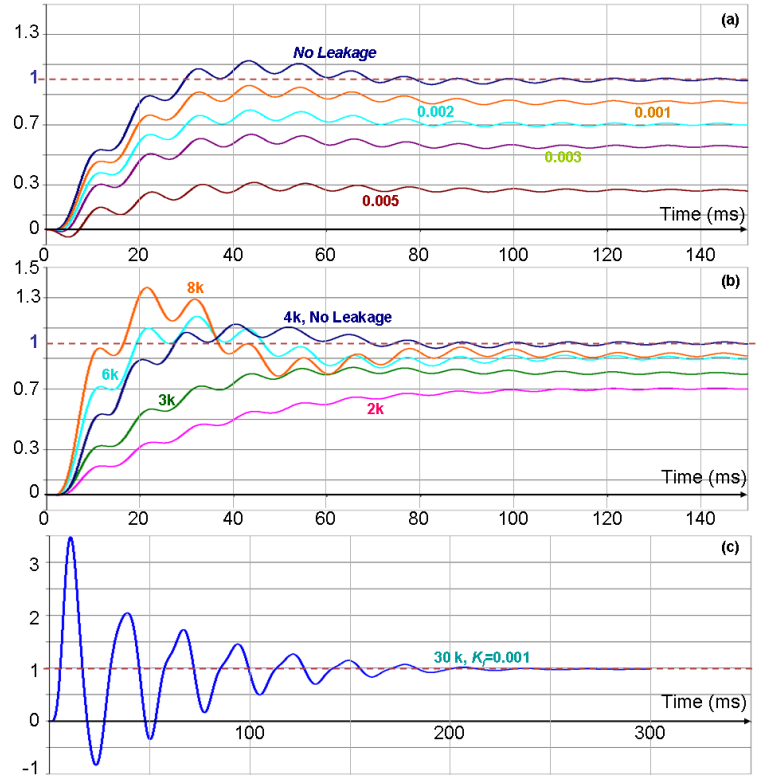


Figure 6: Internal Leakage Effects

pump is also connected with the rod side of the cylinder to prevent possible cavitations. Since only one port of the servo valve is used, the square root of the valve pressure differential is divided by 500 psi, namely  $\Delta P_o = 500$  psi. In addition, if both of the servovalve ports are used, then  $\Delta P_o$  becomes 1000 psi, which reduces the flow rate about 40%.

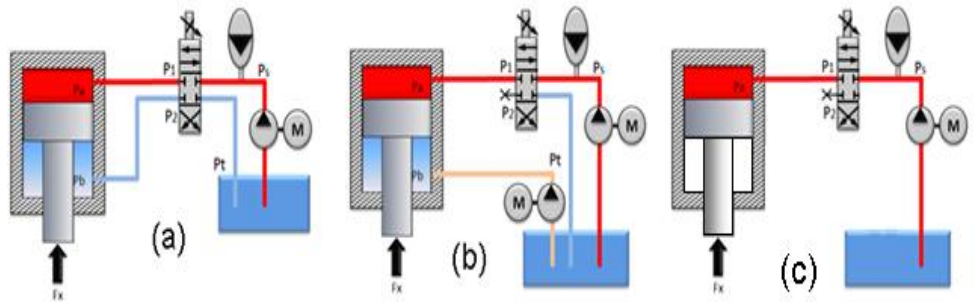


Figure 7: Three Typical HAGC Piping Systems

This section is dedicated to study on the responses of three different piping systems as shown in Figure 7. Figure 7c shows the simplest design, which does not contain any oil on the rod side. The oil in the piston side is charged and discharged through the servo valve. No return line is required. Figure 7b has the oil on the rod side, but it has no interaction with the piston side oil. The oil is pushed back to the tank when the piston moves downward and sucked back to the rod side when the piston moves upward. There is an auxiliary pump or a pressure regulating valve to maintain a positive gage pressure at the tank side to prevent from pipe line vacuum due to the piston suction. Previous results were obtained based on this piping system. Figure 7a is designed to connect the returning line back to the same servo valve so that the cylinder will have one side charging and the other side dumping. At a first thought, this system will accelerate the system response due to the double action within a certain application. For the first system, there is a transmission line from the rod end to the B port of the servo valve. For convenience, this section will not consider transmission lines, namely, equations (4) and (5) will not be applied and  $P_a=P_b$ . Equation (7) is also not applicable for the first piping system (a). All equations are applicable for the second piping system. As to the last system, equation (7) is eliminated and other equations except (4) and (5) remain the same.

Furthermore, this section will investigate the effects from various area ratios. The area ratio is defined as the area ratio of the piston side to the rod side. For the mill application, the area ratio ranges from 1.15 to 7.5 depending on the cylinder design. The cluster mill provides a large mechanical advantage of about 1:25. Namely, the AGC cylinder takes only about 4% of the separation force. Hence, the cylinder is small and the ratio is around 1.15 for the cluster mill. For the pancake or tandem cylinders, the cylinder is larger and the area ratio can be as large as 7.5. The area ratio and the piping system affect the selection of the servo valve size and the current gain factor.

Three area ratios – 1:1, 2:1, and 6:1 – are used here for comparison. The current gains are 4000 for cases (a) ~ (c) and 1000 for case (d). Besides of varying above parameters and designs, some parameters used in this investigation are  $P_s=5000$  psi,  $P_t=200$  psi (if applied),  $P_{a0}=2600$  psi,  $P_{b0}=200$  psi (if applied),  $A_a= 415$  in<sup>2</sup>,  $x_0=1$ ”, and  $L_p=0$  while other parameters remain the same.

Figure 8 shows the frequency response curves for three piping systems and three area ratios with a fixed frequency of 5 Hz and 1-mil amplitude. All four charts have the same x and y scales. The blue curve represents the case of the first piping system, the green curve is for the second, and the grey curve (cannot be seen since it is hidden behind the green curve) is for the third piping system. Figures 8a~8c show the results of using a current gain of 4000. As seen in Figure 8a, for area ratio=1, all three piping systems have very stable responses. The second and third piping system has better response than the first one. Figure 8b shows similar results even with a larger area ratio of 2:1. For a large area ratio of 6:1, Figure 8c shows the second and third systems have nearly the

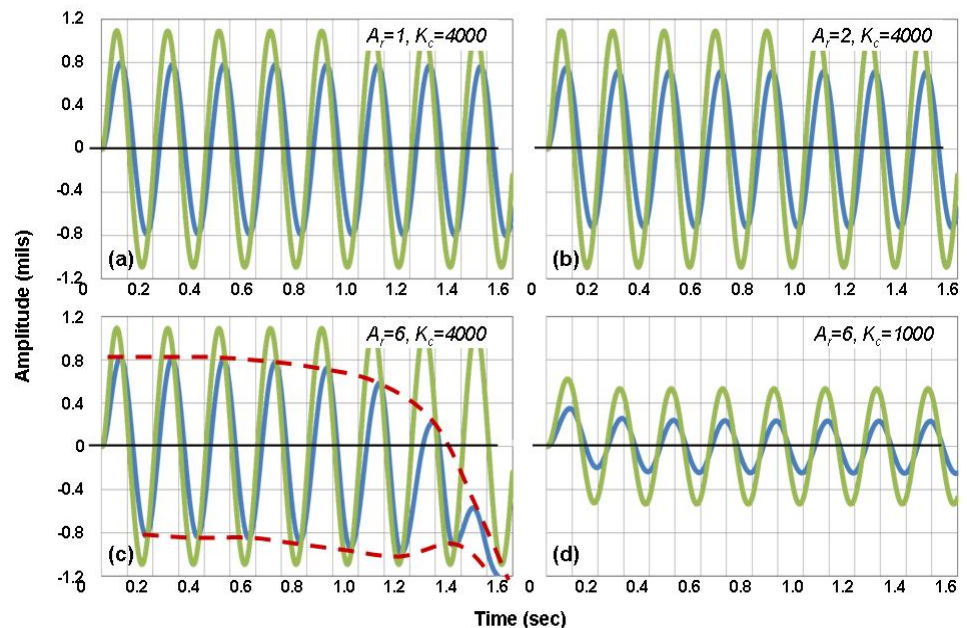


Figure 8: 5 Hz Frequency Responses of Three Piping Systems

same performance and are very stable. However, for the first system, the response curve moves downward after five cycles and becomes unstable (not shown in Figure 8). The simplest way to coup with this situation is to detune the servo vale to have a much smaller current gain factor. Figure 8d shows that a smaller current gain of 1000 brings the first system back to a stable condition although the responded amplitude is reduced as well. The second and third systems also show less performance with the smaller current gain.

Figure 9 displays the Bode charts for three piping systems and three area ratios. For a small area ratio, all systems are very stable. The responses of the second (curves 2 and 5) and third (curves 3 and 6) systems have different curves even their curves are nearly the same in Figure 9. As shown before, the curve 2 has a natural frequency about the mill frequency of 64 Hz. Curve 3 has nearly the same trend as curve 2 before the cross over point of 15 Hz, then its amplitude decays faster than curve 2. Curve 3 actually pushes back the natural frequency to be higher than 100 Hz. Curve 1 has the slowest response at the low frequency although it can be compensated by increasing the current gain as long as the system remains stable. Observing the trend of curve 1, one can expect that curve 1 pushes the natural frequency to be even larger than curve 3. Namely, the curve 1 of the first piping system has the highest first natural frequency. This could be a benefit of using the first system.

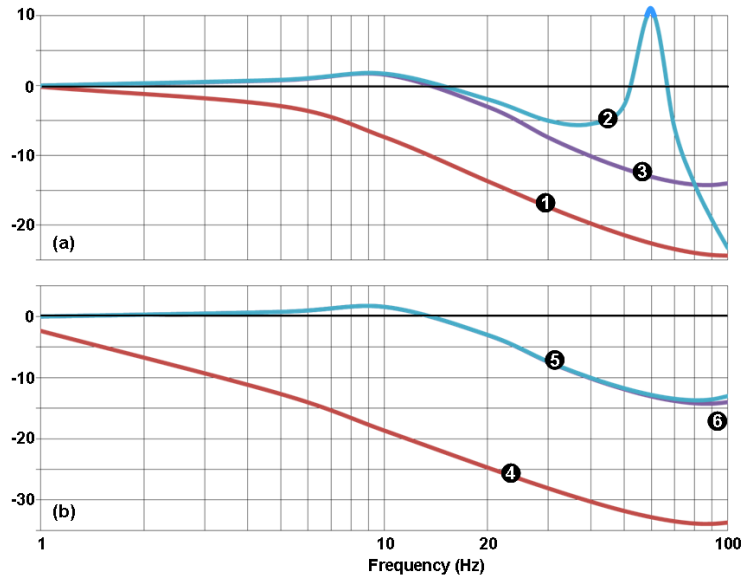


Figure 9: Bode Charts for Three Piping Systems

Since the first system cannot be stable with a larger area ratio of 6, Figure 9b shows two curves 5 and 6 with a current gain of 4000 and curve 4 with a current gain of 1000 so that all three cases are stable. Again both 5 and 6 are identical at the low frequency range and have a very small difference when the frequency reaches 100 Hz. Comparing Figure 9a and 9b, the response curves for the third piping system are identical because the rod side has no oil and no back pressure to provide any counter force to the system. As to the curves 2 and 5 for the second system, the natural frequency of the higher area ratio becomes higher than 100 Hz with about the same frequency response. Hence, the area ratio does not have any significant effect on the second and third piping systems. As shown in curve 6 of Figure 9b, the smaller gain in the first piping system stabilizes the system response, but attenuates the response magnitude. Consequently, the first piping system is not recommended for the system with a large area ratio.

As mentioned before, the cluster mill needs small cylinders with small servo valves thanks to its large mechanical advantage. The natural frequency of the mill is higher than the vertical stack mill thanks to its very rigid mill modulus and extremely compact design. The AGC control of the cluster mill can be referred to the prior art without further discussion here<sup>[25]</sup>. Figure 10 shows the frequency response for a typical cluster mill with the mill information;  $P_s=4000$  psi,  $P_a=2000$  psi,  $P_r=15$  psi,  $A_a=38.5$  in<sup>2</sup>,  $A_b=31.4$  in<sup>2</sup>,  $x_o=0.01$ ”,  $\omega_s=85$  Hz,  $I_o=40$ mA,  $K_c=1200$  mA/in,  $q_{ro}=15$  gpm,  $\omega_m=128$  Hz, and  $k_m=120,000$  k#/in. The blue curve is the result of the second and third piping systems (two curves are nearly identical) while the red curve is for the first one. From the frequency performance viewpoint, the third one is still better than the first one. However, the cluster mill does not have the overbalance system like the vertical stack mill does to empty the oil of the AGC cylinder. The piston retreat relies on the servo valve as well. The first system is considered as the best system for the cluster mill to provide a two-way movement of the AGC cylinder with an acceptable system response thanks to its smallest area ratio.

The pre-stress split housing mill<sup>[26]</sup> has top and bottom housing connected with tie rods and pre-stress cylinders at four corners of the mill. Four spacer cylinders are designed to provide a fixed space between two housings. These cylinders can be used as over balance cylinders if necessary. Therefore, the third (or second) piping system can be applied for better frequency response. Further study may be required to have a deeper consideration.

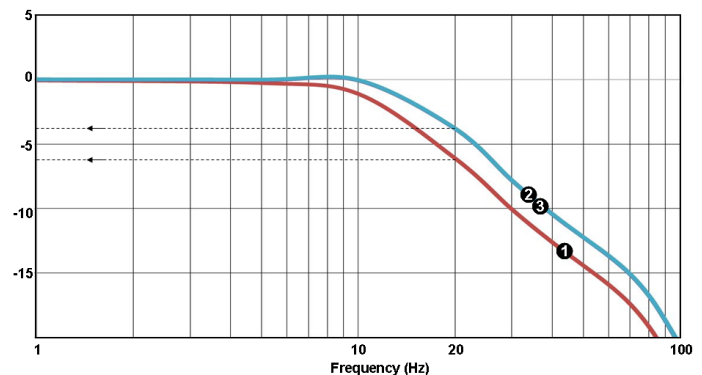


Figure 10: Bode Charts of Different Piping Systems for a Typical Cluster Mill

## CONCLUSION AND OUTLOOK

This article has shown the step and frequency responses of the HAGC hydraulic system. There are nine governing equations for the HAGC system. All equations can be arranged into a block diagram with four shaded non-linear blocks. The software package MetLab was adopted to perform the linear and nonlinear solutions using the block diagram. A closed form transfer function can be derived after three nonlinear equations are linearized and all equations are solved simultaneously. The closed form transfer function can be used as the plant of the linear system to further design the controller in the future. The frequency response of the linear system was shown for various transmission line lengths and initial oil columns. A smaller initial oil column has better response with a larger first natural frequency. The system with larger initial oil column is also stable in the low frequency range. The nonlinear terms make small differences on the system response.

Furthermore, investigation of the system response due to various friction forces, return line lengths, and cylinder internal leakages was performed. The friction force being a damping force can attenuate the responded fluctuation in the step response. The larger the friction force is the smaller the amplitude becomes. On the other hand, the return line should provide back pressure to resist the piston force as a damping force. The study shows that the longer the return line length is the larger the amplitude becomes. However, the longer return line can have a better frequency response although the back pressure cannot be considered as a kind of damping force. The internal leakage through the orifice or the seal of the piston does not help the system response; instead, it leads to a different convergent position. The greater leakage drives the system further away from the target position in the step response test. Even with a larger current gain, the system can approach to the target, but cannot reach the target if the system has any small leakage. The system can nearly arrive at the target with an extremely large gain but the large amplitude fluctuation cannot be acceptable in the system design. As a result, the leakage should be prevented as much as possible. The system performance for three typical hydraulic piping systems and three area ratios were investigated as well. The area ratio plays a very important role in the system response. For small area ratios, the system response is about the same for all three different piping systems. The larger area ratio can push the system toward unstable territory. Detuning the servo valve or replacing with a smaller valve is a solution to bring the system back to stable condition with a certain system performance reduction. The system without oil in the rod side is a simpler design, but this design calls for a higher overbalance force to separate the roll gap since there is no active force in the rod side. The system connecting both sides to the same valve can be applied in the cases of small area ratios only for system stability consideration. The system with a pressurized return line seems to have no particular advantages over the system without oil in the rod side since the return line was found to provide no damping effect in this study.

The continuation of this study will focus more on the linear system from which the controller can be designed to improve the system performance. The rolling mill application prefers the robust control to have a uniform performance for the entire product mix. The optimal control is still possible to have better command follow in the low frequency range and stronger noise rejection in the high frequency range. The qualitative feedback control is another possibility for future investigation. Yet the gain scheduling method is simple, straight forward, easy, and acceptable for most engineers and operators. Hence, the further study on the hydraulic system response should investigate control methods and propose a general method which can be applicable for rolling mill application.

## ACKNOWLEDGEMENT

The authors are indebted to Mr. Jerry Martins for providing vast information on hydraulic system performance and designs. Yet we thank him for reading through this paper and giving us suggestions on the paper. Most importantly, we like to thank Tenova's management team for their R&D support and approval for this paper to be presented and published.

## REFERENCES

- 1) Davies, R. M. and Lambert, T. H., "Transient Response of an Hydraulic Servomechanism Flexibly Connected to an Inertial Load", J. Mech. Engng Sci., 1964, No. 6, pp32
- 2) Nikiforuk, P. N., et al, "The Large Signal Response of a Loaded High Pressure Hydraulic Servomechanism", The Institution of Mechanical Engineers Proceedings, 1965-66, vol. 180, part I, pp 32 -66
- 3) Collinson, C. D., "Hydraulic Gap Control on Strip Rolling Mills", Measurement and Control, vol. 4, 3/1971, pp T35-40
- 4) Paul, F. W., et al, "The Effect of Fluid Line Length On Hydraulic Gap Controlled Cold Rolling Mills", International Conference on Hydraulic, Pneumatics and Fluidics in Control and Automation, April 1976. pp A6-118-131
- 5) Paul, F. W., "A Mathematical Model for Evaluation of Hydraulic Controlled Cold Rolling Mills", 1975, IFAC 6<sup>th</sup> Triennial World Congress, Boston, Mass, Section 53
- 6) Stone, M. D., "Hydraulic Automatic Gage Control Mills", Iron and Steel Year Book, 1973, pp 313
- 7) Yamazawa, K., "Automation of the Mill Plant – Control System of the Cold Mill", IHI Engineering Review, Special Issue, June 1970, pp 17-24

- 8) Davies, J. et al, "Design Criteria Development and Test Activities for 6-Stand Tandem Mill Hydraulic Screwdown System", JISI, July 1972, pp 489-550
- 9) Yamashita, A. et al, "Development of Feedforward AGC for 70" Hot Strip Mill at Kashima Steel Works", The Sumitomo Search, No. 16, Nov. 1976, pp 34-39
- 10) Okamoto, T. et al, "Advanced Gage and Tension Control of Tandem Cold Mill with Hydraulic Screwdown System", Transaction ISIJ, vol. 16, 1976, pp 614-622
- 11) Fapiano, D. J. and Steeper, D. E., "Thickness Control in Cold Rolling", AISE Year Book, 1983, pp 442-452
- 12) Hayama, Y., et. al., "Development of a High Response Type Hydraulic Roll Gap Control System", MHI Technical Review, vol. 19, No.2, July 1983, pp 1-7
- 13) Ginzburg, V. B., "Dynamic Characteristics of Automatic Gage Control system with Hydraulic Actuators", AISE Year Book, 1984, pp 75-83
- 14) Huzyak, P. and Gerber, T. L., "Design and Application of Hydraulic Gap Control Systems", AISE Year Book, 1984, pp 331-338
- 15) Guo, R. M., "Evaluation of Dynamic Characteristics of HAGC system" Iron and Steel Engineer, July 1991.
- 16) Gao Q. M., et al, "Modeling and Simulation of Hydraulic AGC System for 1100mm Cold Rolling Mill", Applied Mechanics and Materials, vol 34-35, 2010, pp 523-526
- 17) Suisse, B. E., "Research for Dynamic Seal Friction Modeling in Linear Motion Hydraulic Piston Applications" The University of Texas at Arlington, August 2005
- 18) Rath, G., "Model Based Thickness Control of the Cold Strip Rolling Process", Ph. D. dissertation, Dept. of Automation, University of Leoben, Austria, Apr. 2000
- 19) Fuchshumer, S., "Algebraic Linear Identification, Modeling, and Applications of Flatness-based Control", Ph. D. dissertation, Johannes Kepler University, Linz, Dec 2005
- 20) Geyer, L. H., "Controlled Damping Through Dynamic Pressure Feedback", Moog Technical Bulletin, No. 101, 1958, revised 1972
- 21) Guo, R. M., "Analysis of Chatter Vibration Phenomena of Rolling Mills Using Finite Element Methods", Iron and Steel Engineer, Jan 1993, pp 29-39
- 22) Yarita, I., et., al., "An Analysis of Chattering in Cold Rolling for Ultra-Thin Gage Steel Strip", Trans ISIJ, vol. 18, 1978, pp 1-10
- 23) Pawelski, O., et al, "Calculation of the Vibrational Behavior of High-Speed Cold Rolling Tandem Mills", Stahl Eisen, vol. 108, No. 7, 1988, pp 49-54
- 24) "Troubleshooting Hydraulic System Problems", Maintenance Technology International Inc.
- 25) Herbst, F. J., "Rolling Mill Gauge Control System", US Patent 4,244,025, June 1981
- 26) Guo, R. M., "Prestressed Rolling Mill Housing Assembly with Improved Operational Features", US Patent 7,765,844 B2, Aug, 2010